RF-Wise: Pushing the Limit of RFID-based Sensing

Cui Zhao*, Zhenjiang Li†, Han Ding*, Ge Wang*, Wei Xi*, and Jizhong Zhao*
*Faculty of Electronic and Information Engineering, Xi'an Jiaotong University, China
†Department of Computer Science, City University of Hong Kong, China

***Abstract*—RFID shows great potentials to build useful sensing applications. However, current RFID sensing can obtain mainly a single-dimensional sensing measurement from each reader-to-tag query, such as phase, RSS, etc. This is sufficient to fulfill the designs that are bounded to the tag's own movement, e.g., the localization of tags. However, it imposes inevitable uncertainty to many sensing tasks relying on the features extracted from the RFID signals, which limits the fidelity of RFID sensing fundamentally and prevents its broader usage in more sophisticated sensing scenarios. This paper presents RF-Wise to push the limit of the RFID-based sensing, motivated by an insightful observation to customize RFID signals. RF-Wise can enrich the existing single-dimensional feature measure to a channel state information (CSI)-like measure with up to 150 dimensional samples across different frequencies concurrently. More importantly, RF-Wise is a software solution atop the standard EPC Gen2 protocol without using any extra hardware, requires only one tag for sensing and works within the ISM band. RF-Wise, so far as we know, is the first system of such a kind. Extensive experiments show that RF-Wise does not impact underlying RFID communications, while by using the features extracted by RF-Wise, applications' sensing performance can be improved remarkably. The source codes of RF-Wise are available at https://cui-zhao.github.io/RF-WISE/.**

I. Introduction

We have recently witnessed a surge of research that leverages the wireless signals for sensing [1], [2], [3], among which RFID (Radio Frequency Identification) is an important and widely adopted such technique. RFID employs passive tags as the sensors usually [4]. These tags are battery-free, small-in-size and low-cost, which are suitable to achieve a long-term and large-scale deployment for plenty of useful applications in practice, including the food safety [5], the contactless HCI [6], the smart manufacturing [7], etc.

Motivation. RFID reader queries tags following an Aloha-based MAC from the EPC Gen2 protocol [8]. The reading rate (the frequency to collect the sensing samples) is *moderate* merely, *e.g.*, 40∼200 times per sec. Hence, the sensing quality from each query becomes more crucial. However, the current RFID sensing can obtain mainly a *single-dimensional* sensing measurement from each query, such as phase, RSS, etc. This is sufficient for the designs bounded to tag's own movement, *e.g.*, the localization of tags [9], vibration counting [10], etc., while it imposes inevitable uncertainties to a large spectrum of sensing tasks relying on the detailed features extracted from the RFID signals, *e.g.*, to recognize the diluted alcohols or fake/expired food materials with subtle differences to ensure the food safety [1], to capture fast or subtle gestures for the contactless human-computer interactions [11], to sense dense goods in the manufacturing, etc., which thus limits the fidelity of RFID sensing fundamentally and prevents its broader usage in more sophisticated and realistic sensing scenarios.

To overcome these limitations, great efforts have been made to increase the sensing sample's *diversity* by using frequency hopping [12] or tag array [13], which however are not effective due to the inherently large latency between two sample collections (Section VI). Some recent work [1] proposes to utilize an extra device to transmit additional wide-band (500 MHz) signals to improve the sensing fidelity. The cost (from the extra transmission device) and overhead (to synchronize this extra signal with the RFID signal) cannot be neglected. We thus wonder naturally *whether we can improve RFID sensing without such extra costs and overhead?*

Observation. The system proposed in this paper, RF-Wise, brings a positive answer. It can enrich the single-dimensional sensing measurement to a fine-grained channel state information (CSI)-like measure, composed of a series of independent sensing samples obtained across frequencies. RF-Wise can further enhance this sensing fidelity by harnessing more usable bandwidth in RFID. More importantly, RF-Wise is a purely software solution atop the standard RFID system without using any extra hardware. It requires only one tag for sensing, works within the ISM band, is compatible to the EPC Gen2 protocol and is a generic design to be integrated into many existing applications to improve their performance directly. RF-Wise is designed based on the following observation.

The RFID signal contains a *continuous wave* to power tag's backscattering, which is configured with a constant amplitude value usually. In this paper, we observe that the tag's backscattering is not sensitive to the *waveform format* of the continuous wave — even it is designed to be another type of sequences with enough energy, tags may still be activated and functioned normally. This observation inspires us to "customize" the continuous wave by employing the frequency multiplexing, so that we can collect multiple sensing samples over frequencies concurrently from each query (no frequency hopping). For example, the sensing dimension can be increased from 1 to 16 to fully cover the typical 2 MHz band with a frequency spacing of 125 KHz. Moreover, improved by using more allowable or usable bandwidth in RFID, *e.g.*, 26 MHz in U.S., the sensing dimension can be increased up to 150 further, which thus fundamentally breaks the limit in the current RFID sensing.

However, to realize this idea in a real system, we need to address the following three challenges.

1) Protocol-compatible frequency multiplexing. Frequency multiplexing is a mature wireless technique, *e.g.*, in Wi-Fi [14]. But, to enable it for RFID, we need to ensure the RFID signal

still adheres to the EPC Gen2 protocol after our customization, such that RF-Wise is compatible to the off-the-shelf tags and does not impair the inherent RFID communications.

2) Hardware imperfection and constraints. To take a full advantage of frequency multiplexing, we observe a severe and unique cascaded integrator-comb (CIC) roll-off issue [15] as well as other hardware constraints. They can be avoided with the bandwidth commonly adopted in the RFID communications, while they appear when more bandwidths are expected to use for sensing. We should address them explicitly.

3) Feature extraction. Finally, we need to figure out how to extract more representative and reliable features from the sensing samples obtained from our design, so that RF-Wise can benefit a variety of sensing applications directly.

Contributions. In this paper, we propose effective techniques to address above challenges. To validate the efficacy of RF-Wise, we develop a prototype using one USRP X310 software radio with a daughter-board merely, and test it with the off-the-shelf passive tags. The underlying communication still follows the EPC Gen2 protocol without impacting its communication efficiency, while the dimension of the sensing samples from each query can be improved up to 150. With such an enhanced sensing ability, we investigate its utility through *liquid classification* and *gesture recognition* two concrete applications, and observe the performance gain from 20.2% to 40.7% by replacing the sensing features derived from RF-Wise.

Meanwhile, we have also made great engineering efforts to upgrade the public EPC Gen2 source code [16] to support RF-Wise with several promising new features: 1) I/Q modulation for the continuous wave, 2) code optimization to avoid "core dumped error", and 3) parameter configuration to enable a wider-band RFID transmission of up to 25 MHz. So far as we know, no such codes are publicly available yet and we release our codes in [17] to facilitate the future studies. In summary, this paper has made the following contributions:

- To our best knowledge, RF-Wise is the first work to obtain fine-grained CSI-like sensing samples purely from RFID signals to advance RFID sensing. It is a software solution atop standard RFID without using any extra device, compatible to EPC Gen2 within ISM band, requires one tag for sensing and is generic for various applications.
- We identify a series of unique challenges encountered in designing RF-Wise. We propose novel and effective techniques to address these challenging issues.
- We make great engineering efforts to the system development. We examine RF-Wise's efficacy by two applications. Results also suggest RF-Wise does not impact the efficiency of the underlying RFID communications.

II. Preliminaries

A. Application Scenarios

In this section, we first discuss the application scenarios that RF-Wise can benefit, including at least:

1) Food safety. Sensing foods or materials in a non-invasive way is a promising and important topic to ensure the food safety. For instance, the diluted alcohols mixed by the cheap methanol could lead to blindness or even death of people [18]. Fake materials (*e.g.*, oil, medicine, etc.) could cause allergy or other diseases [19]. Expired drinks may also cause health issues. To sense foods using RFID, the features are generated by the coupling effect between the food and the tag [20], which can be reflected at different frequencies. RF-Wise can extract such fine-grained features to enable a reliable sensing.

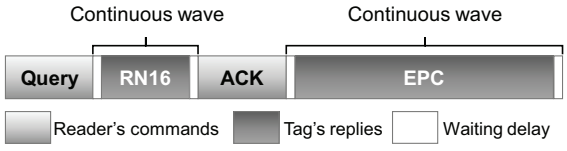

Fig. 1. Illustration of each RFID query in one inventory.

2) Contactless HCI. Contactless human-computer interactions (HCI) become increasingly desired nowadays to reduce the risk of influenza infection. For instance, in public lavatories, users can use their hand gestures in the air to operate the automatic toilet system to avoid a physical touch. At gate entrances, the user's gesture or speaking features can be used for authentication [21], without removing face masks or typing on the input panel. For these applications, the features from the dynamic gestures can be captured more precisely through the sensing measures of RF-Wise cross different frequencies.

3) Smart manufacturing. RFID sensing can also be applied to achieve the smart manufacturing and industry management, *e.g.*, deciding whether the fragile goods are placed slantingly, recognizing worker' gestures in the air to operate the devices deployed in remote, hash or even dangerous areas, etc.

B. RFID Communication Primer

Before elaborating the system design, we introduce RFID communication primer. RFID reader queries tags in an inventory basis following the EPC Gen2 protocol, as Fig. 1 shows.

- Reader starts with a "Query" command and waits for the "RN16" reply backscattered by the tag. During this waiting interval, reader transmits an unmodulated radio frequency (RF) carrier, which is the **continuous wave**, to power the tag's backscattering for the "RN16" reply.
- After "RN16" is received, reader continues to transmit continuous wave for tag to backscatter its "EPC".

Before introducing our design, we make the following two notes to facilitate the discussions in the rest of this paper:

- *Query*: For the representation ease, the term "query" in the rest paper refers to the whole inventory, instead of the "Query" command (Fig. 1) unless specified otherwise.
- *Continuous wave*: For each query, prior sensing samples (*e.g.*, phase, RSS, etc.) are extracted from the "EPC" field in the received signal. We also adopt this field. Hence, our proposed signal operations in next section is only applied to the continuous wave covering the "EPC" field.

III. RF-Wise Design

RF-Wise contains three main components shown in Fig. 2:

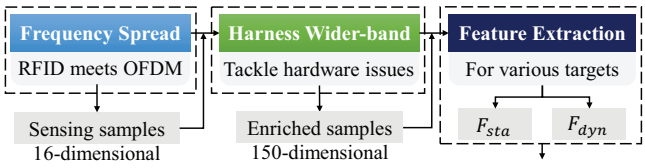

Fig. 2. The overview of the RF-Wise design.

- **Frequency spreading** (Section III-A): multiplexing frequencies by customizing continuous wave to obtain multi-dimensional sensing samples from different frequencies.
- **Harnessing wider-band** (Section III-B): harnessing more usable bandwidth to enrich the sensing samples further, and enhance the timing resolution of sensing as well, after a set of the hardware related issues are addressed.
- **Feature extraction** (Section III-C): extracting representative and effective features from the sensing samples obtained by RF-Wise, to be used by various applications.

Next, we elaborate the design of each component in RF-Wise.

A. Multi-carrier Frequency Spreading

In each query, **continuous wave** (denoted as s) is modulated to the carrier wave to provide sufficient energy to activate tag's backscattering, and s is set with a *constant* amplitude usually.

Opportunity. Through our study, we find tag's backscattering is *not sensitive* to the *waveform format* of s. Even s is designed as other type of sequences, when it is strong enough, tags may still be activated and functioned normally. We illustrate this observation in Fig. 3 (test-bed setup is detailed in Section V), in which s is designed as a repeated random sequence. For a clear observation, we customize (or modify) s for the left part only and leave the right part as the standard constant s. Fig. 3 shows that reader can still receive the tag's EPC reply. Compared with the EPC received with the standard s, the left-part EPC reply contains some jags, while the EPC bits from both parts can be decoded correctly by the RFID reader.

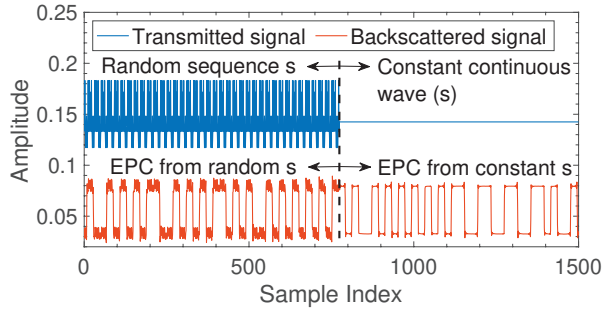

Fig. 3. Tag's backscattering is not sensitive to the waveform format of s.

This observation offers a chance to "customize" s to enrich the sensing dimensions for each query dramatically — We propose to multiplex the frequency of s to build orthogonal sub-carriers in parallel, so that *independent* and *multi-dimensional* samples can be obtained from these sub-carriers concurrently in each query. For example, with a sub-carrier spacing of 125 KHz and a typical 2 MHz bandwidth, we can obtain 16 ($= \frac{2\ MHz}{125\ KHz}$) samples from each query to cover this 2 MHz band, which is similar as the channel state information (CSI) measure in Wi-Fi [22]. This signal customization is purely software based without using any extra hardware. To build sub-carriers for RFID, we adopt the orthogonal frequency-division multiplexing (OFDM) under the RFID-incurred constraints.

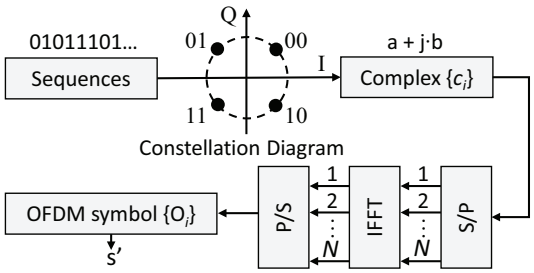

Fig. 4. Illustration of the OFDM symbol generation.

Continuous wave meets OFDM. We first introduce our OFDM symbol generator as shown in Fig. 4, followed by two issues that need to be addressed in the context of RFID.

- A dummy binary sequence is generated and mapped on a constellation diagram to produce OFDM symbols using PSK (phase-shift keying) of degree n, *i.e.*, the constellation diagram contains n points in total and every $\log_2(n)$ dummy bits are mapped to one constellation point. Fig. 4 shows the case when $n = 4$. Each constellation point i is a complex number c_i in the frequency domain and a series of $\{c_i\}$ are generated from the dummy sequence.
- The complex numbers $\{c_i\}$ then go through three routine modules — Serial-to-Parallel (S/P), Inverse Fast Fourier Transform (IFFT) and Parallel-to-Serial (P/S). For IFFT, every N complex numbers c_is are grouped to perform IFFT, where N is the IFFT length and it also equals to the number of sub-carriers to occupy different frequencies. Finally, after the "P/S" module, each group of N complex numbers c_is produce one piece of the signal in the time domain, which is one **OFDM symbol** O_i. All the OFDM symbols together form the new continuous wave s'.

Problem. Above OFDM generation is inspired by the frequency multiplexing in Wi-Fi, whereas to apply it for RFID, we need to ensure that the customized s' is still compatible to the standard RFID EPC Gen2 protocol and hardware.

1) OFDM symbol length. RFID tag backscatters a reader's query using the "ON/OFF" keying (OOK) modulation. During the switch of these two opposite states (Fig. 5), a significant signal fading occurs. So, within each "ON/OFF" state, at least one **complete** OFDM symbol should not cross the switching edge of two states. It can be ensured by setting the sub-carrier number N (in Fig. 4) to obtain a proper symbol length.

For RFID, the number of the signal samples in one "ON" or "OFF" state (denoted as M) is determined by both the bandwidth B and the backscatter link frequency (f_{BLF}) [23]:

$$M = B/(\mu \times f_{BLF}) = B \times P_{TRcal}/(\mu \times P_{DR}), \quad (1)$$

where $\mu = 1$ or 2 according to from which bit(s) the OFDM symbols are extracted (detailed in Section III-C). Moreover, $f_{BLF} = P_{DR}/P_{TRcal}$, and P_{DR} and P_{TRcal} are two RFID

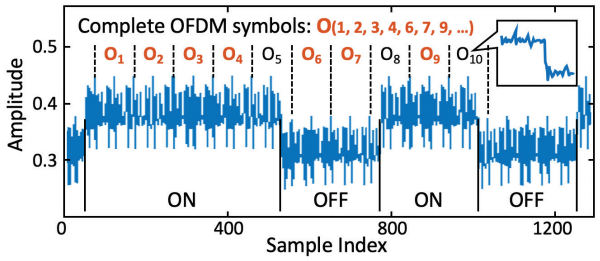

Fig. 5. To ensure at least one complete OFDM symbol in each "ON/OFF" state, the OFDM symbol length should be no greater than half of the state's.

system parameters.[1] To ensure that at least one complete OFDM symbol is in each "ON" or "OFF" state, the OFDM symbol length should be no greater than half of the "ON" or "OFF" duration. In other words, the number of samples from one OFDM symbol (N) should be less than or equal to half of the signal samples (M) in one "ON" or "OFF" state as follows, and Fig. 5 shows one example.

$$N \quad \leq \quad \frac{M}{2} = B \times P_{TRcal}/(2 \times \mu \times P_{DR}) = \tilde{N}. \quad (2)$$

For RFID sensing, a larger N is desired, such that more sensing samples can be collected from more different sub-carriers. However, Eq. (2) indicates that the increasing of N cannot exceed an upper-bound $\tilde{N}$ due to "OOK" modulation; Otherwise, the quality of the OFDM symbol cannot be guaranteed. The specific value of $\tilde{N}$ depends on B, P_{TRcal} and P_{DR}, whose setting will be discussed in Section III-B.

2) Coexisted sensing and communication. The new continuous wave s' obtained so far complies to RFID's modulation. However, we find that the average energy of this new s' itself is small, which cannot activate tags and the sensing cannot be conducted. To overcome this issue, if we scale s' with a large factor α directly, its energy could be sufficient, while we observe that this scaled continuous wave $\alpha \times s'$ will be too noisy and sacrifices the underlying RFID communication, so that RFID reader cannot decode the tag's replied EPC data.

Therefore, in RF-Wise, we propose to *load* the generated s' on top of the standard constant continuous wave s, instead of replacing it. In such a composed $\overline{s}$ ($= \alpha \times s' + s$), s provides sufficient energy to power tag and s' (with a strength factor α) is employed for sensing, while we need to ensure the *orthogonality* of all the sub-carriers, so that the sensing can be performed correctly atop such a new $\overline{s}$. To this end, for any sub-carrier j, we calculate $\int \overline{s} \times cos(j\omega t)\ dt$ as

$$\begin{aligned} & \int (\alpha \times \sum\nolimits_{i=1}^{N} c_i \times cos(i\omega t) + s) \times cos(j\omega t)\ dt, \\ = \quad & \alpha \times c_j \int cos^2(j\omega t)\ dt, \end{aligned} \quad (3)$$

where only the component of sub-carrier j is preserved. Since j refers to the index of any sub-carrier, Eq. (3) indicates the orthogonality among all the sub-carriers. The coexistence of sensing and communication can be thus ensured.

3) Sensing sample extraction. With the injected OFDM symbols, we are able to measure the channel frequency response (CFR, denoted as H_i) from each complete OFDM symbol $\tilde{O}_i$ in the received (EPC) signal by $\tilde{O}_i = H_i \cdot O_i + e$, where O_i is this OFDM symbol before transmission and e is a noise. We can estimate H_i by mean square error minimization [24]. Each H_i is a N-dimensional vector essentially, $H_i = \{h_i(j)\}_{j=1}^{N}$, where each $h_i(j)$ corresponds to one sub-carrier j and N is the total number of sub-carriers. We note that each H_i measured from an OFDM symbol is similar as each CSI measured from a packet in Wi-Fi. Hence, the raw sensing samples $\mathcal{H}$ outputted by RF-Wise from each query are the following set:

$$\mathcal{H} \quad = \quad \{H_i\}_{i=1}^{S}, \quad (4)$$

where S is the number of complete OFDM symbols O_is extracted from this query. Eq. (4) suggests that

- RF-Wise expands the sensing sample's dimensions across frequencies (each H_i is N-dimensional) and this is where the sensing performance gain mainly comes from.
- It can also do such fine-grained sensing multiple times in each query (*e.g.*, $H_{1\sim S}$) to make sensing more reliable.

Later, we propose two types of features derived from $\mathcal{H}$ (Section III-C), which are tailored for different sensing scenarios and can be adopted by different applications directly.

B. Harnessing Hardware-constrained Wider-band

Before elaborating the detailed feature designs, we propose to harness wider bandwidth to further augment $\mathcal{H}$ first. Since the number of bits backscattered by tag in each query is small, *e.g.*, 96–128 bits for EPC, the bandwidth used for RFID communications is relatively narrow usually (1∼2 MHz), while the total *allowable* or *usable* bandwidth for RFID communications is much wider, *e.g.*, 26 MHz (U.S.), 8 MHz (Australia), 5 MHz (China), etc. This inspires us to further spread OFDM symbols to occupy more bandwidth to obtain more concurrent samples from each query, *e.g.*, with the bandwidth of 25 MHz, each H_i can produce 150 samples over this band. On the other hand, a wider bandwidth can increase the timing resolution of each H_i further ($\Delta t \propto 1/B$, the smaller the better). This is beneficial, especially for capturing the object's or human's mobility.

Problem. Within an allowable bandwidth upper-bound (B_u), we find that the bandwidth B may not be able to simply set as B_u, since an inappropriate B will cause a serious cascaded integrator-comb (CIC) roll-off issue [15] and other hardware problems to "pollute" the transmitted signal and undermine the sensing. This is a unique challenge when more bandwidths are leveraged in the RFID sensing.

Formulation. CIC filters are a class of finite-response filters, used in both the RF signal transmitting and receiving [25]:

- *Transmitting*: they are the anti-imaging filters to interpolate signals for increasing the sample rate.
- *Receiving*: they are anti-aliasing filters to decimate signals for reducing the sample rate.

[1]Tag measures the duration of P_{TRcal}, which is contained in the preamble of the reader's query. Meanwhile, P_{DR} is set to either 8 or 64/3 merely in RFID, which is indicated by one bit in the query command as well. Tag then knows $f_{BLF} = P_{DR}/P_{TRcal}$ for backcattering.

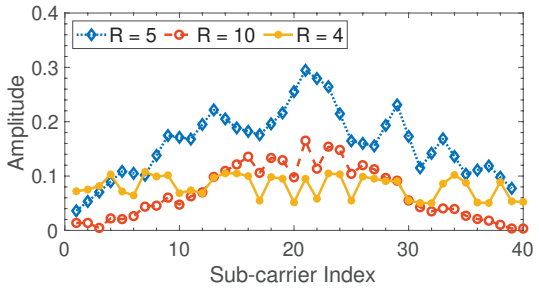

Fig. 6. The CIC roll-off issue occurs severely when the ratio R is odd, then becomes moderate (R is even) and disappears (R is power of 2). In the last case ($R = 4$), the frequency responses, reflecting the sensing target's impact, are usable, which are not impaired by the strong peak due to the roll-off issue.

The purpose to perform interpolation or decimation is to bridge the rate mismatch between the sample rate (whose value equals to the bandwidth B) and the DAC/ADC rate r (r is fixed and equals to 100/200/400 MHz normally). In the CIC filters, there is a key ratio $R = \frac{r}{B}$ to be determined for avoiding the CIC roll-off issue. To this end, we consider the following aspects:

- First, to ensure RFID to communicate normally, the ratio $R = \frac{r}{B}$ needs to be an *even* number according to the hardware characteristic [26]. Otherwise, a strong response will always appear around the central frequency to dominate the signal and undermine the sensing. However, for our sensing design, we find that an even number may not be enough and R should be further in a form of 2^i, where i is a positive integer, as Fig. 6 depicts. In traditional RFID communications, B is 1∼2 MHz usually, satisfying R's requirement thus without suffering the CIC roll-off issue.
- On the other hand, the value of bandwidth B also impacts the feasible range of other RFID meta parameters θ_B, including f_{BLF}, P_{TRcal}, P_{Tari}, etc. These parameters together decide the lengths ($L_j(\cdot)$) of "Query", "RN16", "ACK" and "EPC" these four fields, which must be integers ($\in N_+$). For instance, the length for EPC can be computed by $L_{EPC}(\cdot) = (t_1 + t_2 + t_{epc} \cdot 10^6 / f_{BLF}) \cdot B/10^6$, where t_1 and t_2 are the waiting delays before and after the duration of EPC t_{epc}.

With above understanding, the solution can be formulated as maximizing bandwidth B subjected to hardware constraints:

$$\max_{\{\theta_B\}} \ B, \tag{5}$$

$$s.t. \quad B \le B_u, \tag{6}$$

$$\frac{r}{B} \in \{2^i\}, \ i = 1, 2, \ldots, \tag{7}$$

$$L_j(B, \theta_B) \in N_+, \ j = 1, \ldots, 4, \tag{8}$$

where Eq. (6) ensures that the B is in an allowable bandwidth range, Eq. (7) avoids the CIC roll-off issue and Eq. (8) ensures all the lengths to be integers. By solving this problem, we can determine B and leverage this wider bandwidth to augment each H_i in $\mathcal{H}$ to include the sensing samples from more frequencies. Meanwhile, above constraints also ensure that the underlying RFID communications are not impacted.

As Fig. 7(a) shows, if we simply adopt a wider bandwidth without our frequency multiplexing design, only the central frequency is strong and other frequency components are too weak to be used for sensing. In contrast, with RF-Wise, the entire band is strong enough for sensing, as Fig. 7(b) depicts.

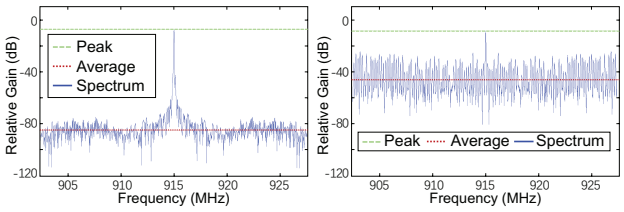

(a) With constant continuous wave s (b) With our customized $\bar{s}$

Fig. 7. Comparison of spectrum utilization over a wider-band of 25 MHz.

C. Sensing Feature Extraction

In Section III-A, we obtain the sensing samples $\mathcal{H}$ ($= \{H_i\}$) from each query, and H_i is the channel frequency response from each complete OFDM symbol i. Through our study, we find that due to the OOK modulation, the "ON"/"OFF" state lasts for *a half of* or *a whole* bit length for bit "0" or "1", respectively, as shown in Fig. 8. There are thus two different formats of H_i when OFDM symbols are obtained from different bits with different merits as discussed below.

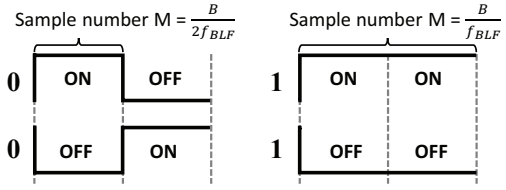

Fig. 8. Duration of the "ON"/"OFF" state for bit "0" and "1", respectively.

1) $\mathcal{H}^1$ *(*$= \{H_i^1\}$*)*, where OFDM symbols are obtained from bits "1" only. In this case, the upper-bound $\tilde{N}$ for the number of sub-carriers is larger (*i.e.*, the factor $\mu = 1$ in Eqs. (1) and (2)) compared with $\tilde{N}$ in the next case.

The advantage to collect OFDM symbols from only bits "1" is that each H_i^1 contains the sensing samples from more sub-carriers, *e.g.*, finer-grained samples across frequencies, while the drawback is that there are no sensing samples from bit "0", leading to some "empty" sensing spots along the time in the received (EPC) signal. Fortunately, to sense static targets (*e.g.*, liquid recognition), the frequency granularity dominates the sensing performance rather than the number of H_is. Therefore, if RF-Wise is deployed to sense static targets, we propose to configure RF-Wise to collect $\mathcal{H}^1$ from bits "1" only and then derive the following feature from $\mathcal{H}^1$ for applications:

$$\mathcal{F}_{sta} \ = \ \frac{1}{q_1} \sum\nolimits_{i=1}^{q_1} H_i^1(on) - \frac{1}{q_2} \sum\nolimits_{j=1}^{q_2} H_j^1(off), \tag{9}$$

where q_1 and q_2 are the numbers of OFDM symbols identified from the "ON" and "OFF" states for bits "1" in each query, respectively. As $H_j^1(off)$s capture the features from the environment only, the subtraction can help remove some impact from the environment [27] and focus more on the static sensing target. Feature $\mathcal{F}_{sta}$ is a N-dimensional vector and we use it for the liquid classification application in our evaluation.

2) $\mathcal{H}^{0/1}$ *(*$= \{H_i^{0/1}\}$*)*, where OFDM symbols are obtained from both "0,1" bits. Because the state duration of bit "0" is

only half of that of bit "1", in this case, we have to set $\tilde{N}$ to be half of the $\tilde{N}$ above (*i.e.*, by setting $\mu = 2$ in Eqs. (1) and (2)), and the actual number of sub-carriers N' also becomes smaller. However, the advantage is that there will be always two $H_i^{0/1}$s obtained from each bit (no empty sensing spots), which is suitable to sense the moving targets, *e.g.*, the hand gestures. So, if RF-Wise is used to sense dynamic targets, we propose to collect $\mathcal{H}^{0/1}$ and treat it as the feature directly:

$$\mathcal{F}_{dyn} \quad = \quad \mathcal{H}^{0/1} = \{H_i^{0/1}\}_{i=1}^{q_3}, \tag{10}$$

where q_3 is the number of OFDM symbols identified from each query in total. Feature $\mathcal{F}_{dyn}$ is a set of N'-dimensional vectors to better capture target's subtle temporal varying, which is used for the gesture recognition in our evaluation.

We note that $\mathcal{F}_{sta}$ and $\mathcal{F}_{dyn}$ introduced above are two examples for two typical sensing scenarios merely. Users are not forced to use them, which can be modified or even re-designed according to the particular sensing requirements.

3) Summary: In summary, RF-Wise is configured by the following two steps for a sensing application:

- After the formulation from Eqs. (5) to (8) is solved, we can first determine the bandwidth B and other meta parameters to ensure RFID's communications.
- Factor μ (in Eqs. (1-2)) is then determined based on the sensing scenario: static ($\mu = 1$) or dynamic ($\mu = 2$), so that a suitable feature can be adopted, *e.g.*, $\mathcal{F}_{sta}$ or $\mathcal{F}_{dyn}$.

IV. Implementation

A. Experimental Setups

Hardware. RF-Wise is developed using one USRP X310 with one SBX-40 daughterboard. Two directional antennas (Laird S9028PCR with the gain of 8 dBi) are installed to transmit and receive signals to and from the Alien 9640 RFID tag, respectively. USRP is connected to a desktop of an Intel Core i9-9900K CPU, 32 GB RAM, Intel Converged Network Adapter X520-DA1 and 10 Gigabit Ethernet Cable for a high bit-rate sensing data collection.

Software development. The back-end of RF-Wise runs on the EPC Gen2 protocol using GNU Radio 3.7 and UHD 3.15 on Ubuntu 18.04. The public native EPC Gen2 source code [16] does not support the modulation of the complex numbers to encode OFDM symbols into the continuous wave. Therefore, we have also made significant engineering efforts to augment this source code, which does not impact its original EPC Gen2 protocol but can support the following new features[2]:

- We enhance the implementation of the Reader Block by adding new codes to process the complex numbers and enable an I/Q modulation for the continuous wave.
- The I/Q modulation with complex numbers will increase the volume of the internal signal data to process (the size of "gr_complex" is twice of the size of float), which will lead to a "core dumped" error. We propose and implement a memory segmentation strategy to address this issue.
- Configuring RFID to work on a wider band, *e.g.*, increased from the common 2 MHz to 25 MHz, is non-trivial. We add new codes to support the adaptation of RFID's meta parameters to harness a wider bandwidth.

According to the Ettus USRP document [28], the previous USRP N210 with a 1 GigE interface and a 40 MHz daughterboard provides a usable bandwidth up to 20 MHz only, which is limited by the 1 GigE interface [28]. We thus augment the EPC Gen2 source code for the more recent X310 platform. So far as we know, no prior work has made the engineering efforts above to bring the complex-number modulation to RFID and fully leverage the wider bandwidth yet without impacting the underlying communication.

B. Parameter Configuration

RFID-specific parameters. To adhere to various RFID bandwidth requirements globally, we adopt three typical bandwidth upper-bound (B_u) settings for the evaluation:

- Large setting $B_u = 26$ MHz, *e.g.*, in U.S.A.
- Moderate setting $B_u = 10$ MHz, *e.g.*, in Australia.[3]
- Small setting $B_u = 2$ MHz, *e.g.*, China, Japan, Europe.

To solve the formulation from Eqs. (5) to (8), we have tried each RFID meta parameter with small discrete value steps and examined all the combinations. For each B_u, the bandwidth B is selected to 25 MHz, 10 MHz and 2 MHz respectively, and other parameters are the same as listed in Table I. We note that for $B_u = 26$ MHz, other parameters may lead to a higher B but will cause system's working unstable. We thus still use the parameters in Table I for $B_u = 26$ MHz as well.

TABLE I
SETTING OF RFID'S META PARAMETERS USED IN RF-WISE. THE CENTRAL FREQUENCY OF RFID COMMUNICATION IS SET TO 915 MHZ.

f_{BLF}	P_{TRcal}	P_{RTcal}	P_{Tari}	P_{T_1}	P_{T_2}	P_{DC}
50 KHz	160 μs	60 μs	20 μs	180 μs	380 μs	90 μs

System-specific parameters. Next, we discuss two parameters used by RF-Wise: the sub-carrier number N and the strength factor α multiplied to our customized continuous wave s'.

After the parameters are obtained for each B_u, for each type of the sensing features to be used (*e.g.*, $\mathcal{F}_{sta}$ or $\mathcal{F}_{dyn}$), we can determine the maximal number ($\tilde{N}$) of sub-carriers that can be adopted. However, we find that it is not necessary to set the sub-carrier number N to $\tilde{N}$, because it will increase the computation overhead unnecessarily. For instance, when $B = 25$ MHz, N can be set up to 250, while when it exceeds 150, the obtained feature diversity for $\mathcal{F}_{sta}$ improves only marginally, as shown in Fig. 9(a). We thus adopt $N = 150$ to balance the sensing performance and computation cost. In Table II, we list the values of N for all the sensing scenarios in our evaluation. On the other hand, we find that α cannot be set excessive large; Otherwise, the continuous wave s' will become too noisy, which will impact the EPC decoding by the reader, as Fig. 9(b) shows. In Table II, we also list the α values adopted in different sensing scenarios in our evaluation.

[2]https://cui-zhao.github.io/RF-WISE/

[3]Bandwidth allowed in Australia is up to 8 MHz, which is not supported by X310 and we adopt a close 10 MHz for the moderate setting in the evaluation.

TABLE II
THE SETTINGS OF N AND α ADOPTED FOR DIFFERENT SCENARIOS.

B = 25 MHz		B = 10 MHz		B = 2 MHz	
$\mathcal{F}_{sta}$	$\mathcal{F}_{dyn}$	$\mathcal{F}_{sta}$	$\mathcal{F}_{dyn}$	$\mathcal{F}_{sta}$	$\mathcal{F}_{dyn}$
N = 150 α = 6	N = 100 α = 5.5	N = 80 α = 5.5	N = 40 α = 3.5	N = 16 α = 2.5	N = 8 α = 1.5

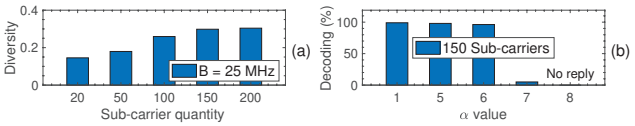

Fig. 9. (a) Feature diversity increases only marginally when N becomes large enough. (b) Large α can impact the decoding rate of the EPC bits.

V. EVALUATION

We evaluate the performance and the utilities of RF-Wise through two useful applications in this section.

1) Liquid classification. As stated in Section II, non-intrusive liquid classification is beneficial to the food safety. In this evaluation, we experiment on 18 different liquids commonly in our daily life, including similar liquids (*e.g.*, coke-pepsi-sprite, beer-wine, skimmed-whole milk, etc.), which are illustrated in Fig. 10(a) and detailed in Fig. 12. For each liquid, we fill it in a plastic container of 200 mL with one tag attached to surface of the container with a thin plastic foam of 1 mm in between (to ensure tag backscatters properly [20]). The antenna-to-tag distance is 50 cm. For each liquid, we collect the sensing data from 250 to 350 times. We then adopt 2/3 of the data to train a classifier (stated below) and the rest data for evaluation.

2) Gesture recognition. Gesture recognition is another useful application to enable contactless HCI. In this evaluation, we invite five users (3 males and 2 females) to conduct the same set of six hand gestures as [29], including to rotate left/right, sweep left/right and zoom in/out. For these gestures, we collect 1200 sensing data in total. We adopt 2/3 of the sensing data for training and the rest for evaluation. The distance between the antennas and the tag is also 50 cm, as shown in Fig. 10(b). We also evaluate RF-Wise under various settings, *e.g.*, different hand-to-tag distances, different speeds to perform gestures, etc.

3) Classifier. To understand the effectiveness of the sensing features obtained from RF-Wise, we adopt a lightweight classifier — the random forest in Weka 3.8.5 [30] — for both applications (without using the advanced neural networks). The four main parameters in a random forest are empirically set as $P = 100$, $I = 100$, $V = 0.001$ and $S = 1$ in evaluation.

A. Performance in Liquid Classification

We compare the following methods in this application:

- **PAR-PHA** [31]: using one pair of tags (PAR) and the signal's phase information (PHA) for sensing;
- **PAR-HOP** [12]: using one pair of tags (PAR) with the mechanism of frequency hopping (HOP) for sensing;
- **ARY-HOP** [13]: using both one tag array of eight tags (ARY) and the frequency hopping (HOP) for sensing;

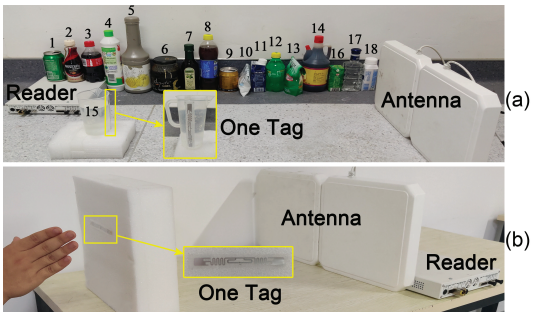

Fig. 10. Setups for (a) liquid classification and (b) gesture recognition.

- **RF-Wise**: our proposed method using only one tag and the $\mathcal{F}_{sta}$ feature ($B = 25$ MHz by default) for sensing.

Overall performance. Fig. 11(a) reports the accuracy among these methods. With the single-dimensional feature from the signal's phase, PAR-PHA cannot classify 18 liquids reliably with an accuracy of 57.5% only. Upgraded by the frequency hopping, PAR-HOP can improve the accuracy to 87.9%. We find that its performance is mainly limited by the large latency between the hopping at any two frequencies, *e.g.*, 200 ms, so that PAR-HOP only hops seven frequencies [12] for an efficient classification. As shown in the next application when the sensing target is moving, such a large latency will degrade the sensing performance significantly. Next, by using eight tags, ARY-HOP further improves the accuracy to 94.6%. In contrast, RF-Wise uses only one tag and achieves the highest accuracy of 98.2%. Compared with PAR-PHA, the fine-grained features from RF-Wise leads to 40.7% gain directly.

Moreover, Fig. 12 shows the detailed confusion matrix of these 18 liquids classified by RF-Wise. We can see that RF-Wise can achieve an accurate classification, which has errors occasionally for the highly similar liquids, *e.g.*, among coke, pepsi and sprite, or between whole and skimmed milks.

Performance v.s. bandwidth. The performance of RF-Wise in Fig. 11(a) is achieved by using the bandwidth of 25 MHz. In Fig. 11(b), we further investigate RF-Wise under other two bandwidth settings. The result shows that even for the common 2 MHz, the fine-grained sensing feature obtained through RF-Wise can lead to a good result already, *e.g.*, 94.8%, which can be further increased to 97.1% when the bandwidth is 10 MHz. Fig. 11(b) indicates that compared with the prior methods, the fine-grained sensing feature across different frequencies is the main source leading to RF-Wise's performance improvement.

Feature's sensitivity. In Fig. 13, we further introduce two more challenging settings intentionally to demonstrate the necessary to use fine-grained features for liquid classification.

In the first setting, we start from the pure wine and add different volumes of water, *e.g.*, 5 mL (2.5%), 10 mL (5%) and 15 mL (7.5%), and show the features obtained by RF-Wise. From Fig. 13(a), we can see that with different volumes of water mixed into the wine, some sub-carriers exhibit distinct frequency responses, which provides an opportunity to distinguish them. This ability can be used to detect the fake wines, *e.g.*, with 5% or more water mixed, RF-Wise can

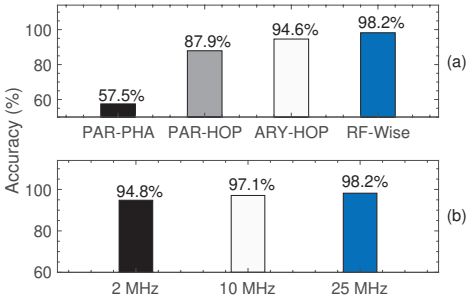

Fig. 11. Classification accuracy (a) among different methods and (b) for RF-Wise using various bandwidths.

	1	2	3	4	5	6	7	8	9	10	11	12	13	14	15	16	17	18	Liquids
1	1																		1 Beer
2		0.95										0.02	0.02			0.01			2 Coffee
3		0.003	0.96					0.017				0.01	0.01						3 Coke
4				0.98										0.007		0.01	0.003		4 Detergent
5				0.01	0.99														5 Juice
6		0.007				0.99											0.003		6 Honey
7							0.99										0.01		7 Oil
8	0.01		0.02					0.96				0.01							8 Pepsi
9				0.003		0.003			0.99				0.003						9 Red Bull
10										0.99			0.01						10 Saline water
11								0.003			0.98					0.017			11 Skimmed milk
12			0.01									0.98				0.01			12 Sprite
13												0.013	0.98		0.007				13 Sweet water
14				0.013	0.007									0.98					14 Vinegar
15	0.01														0.99				15 Water
16					0.003						0.02		0.003			0.97		0.003	16 Whole milk
17																	1		17 Wine
18																		1	18 Yogurt

Fig. 12. The confusion matrix of classifying 18 liquids by RF-Wise using 25 MHz bandwidth with 150 sub-carriers. The names of each liquid are listed in the right column of this matrix.

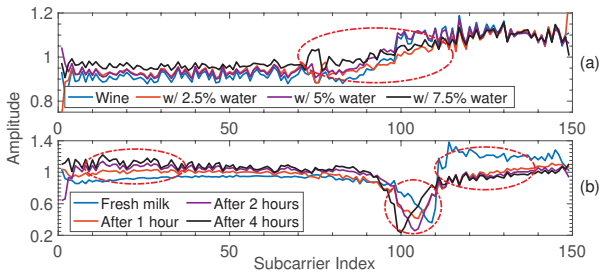

Fig. 13. Sensing features of RF-Wise for (a) the wine by adding different volumes of water and (b) the milk after it is opened for one to four hours.

achieve the accuracy of over 99% to distinguish them.

In the second setting, we open one bottle of fresh milk and collect its sensing features after one, two and four hours (in the environment with a temperature of $30 \sim 35$°C). Fig. 13(b) depicts that their features show differences across sub-carriers and we highlight the most evident parts by the red circles. Both of these two experiments show the importance of fine-grained features to capture the subtle differences for sensing.

B. Performance in Gesture Recognition

In this application, we compare RF-Wise (using one single tag and the $\mathcal{F}_{dyn}$ feature) with PAR-PHA and PAR-HOP as well. For ARY-HOP, we find the large latency in the frequency hopping undermines its sensing performance in the dynamic sensing scenario. Hence, we change it to:

- **ARY-PHA** [29]: using the tag array of ten tags (ARY) and the signal's phase information (PHA) for sensing.

Overall performance. Fig. 14(a) shows the accuracy to recognize six hand gestures by different methods. PAR-PHA achieves the accuracy of 77.3% (which is higher than the accuracy of 57.5% in the liquid classification is because the number of liquids is much larger than that of the gestures). With frequency hopping, the accuracy of PAR-HOP is even decreased and the reason will be explained soon. With the help from multiple tags, ARY-PHA improves the accuracy to 92.9%, while RF-Wise can achieve 97.5% using one tag only. Compared with PAR-PHA, 20.2% gain is obtained by using the RF-Wise's fine-grained features with one tag only.

To understand why the frequency hopping becomes less effective for a dynamic sensing target, we ask a volunteer to perform one gesture three times and Fig. 15(a) shows the features extracted by PAR-HOP each time. The signal actually senses different parts of the gesture each time due to the large and uncertain hopping latency. Moreover, each phase measure leads to a limited number of features to be used. In contrast, the signal from RF-Wise can capture the gesture consistently (without hopping delay) and obtain fine-grained features over frequencies each time (Fig. 15(b)), which thus lead to more reliable sensing result even in the dynamic sensing scenario.

In Fig. 14(b), we further examine the RF-Wise's performance under other two bandwidth settings. The common 2 MHz can lead to 96.1% which will be further increased to 97.2% when the bandwidth is 10 MHz. Such a result also suggests that the high-resolution and fine-grained sensing features are the main source leading to sensing improvement.

Impact of gesture speeds. In the evaluation, we only use the sensing data collected when all the volunteers perform gestures in a normal speed to train the classifier. In Fig. 16(a), we use this classifier to test on the gestures with relatively slower and faster speeds. We can see that the accuracy for both setting is decreased slightly, *e.g.*, 91.7% (slow) and 95% (fast). One possible way to further improve the accuracy is to include a few training data under different speeds. The performance can be improved, *e.g.*, 95.8% (slow) and 96.7% (fast) in Fig. 16(a).

Impact of hand-to-tag distances. So far, we only use the sensing data collected with the hand-to-tag distance of 5 cm to train the classifier. In Fig. 16(b), we use it to examine the performance when the distance is prolonged to 15 cm. It is understandable that the accuracy will decrease when this distance increases, while the accuracy is still above 90% at 15 cm. If we add more training data collected from different distances, the accuracy is consistently high across these distances.

C. Micro-benchmarks

Compatible to RFID communication. To understand whether RF-Wise impacts on the underlying RFID communication, we conduct a series of micro-benchmarks in this subsection. For a comprehensive understanding, we add two more bandwidth settings of 4 and 20 MHz in this experiment. For each micro-benchmark, we use the performance by running the native EPC Gen2 protocol over a common 2 MHz band as a baseline.

Fig. 17(a-c) summarizes the comparison results for 1) the reader's reading rate of RFID tags, 2) the success decoding rate of tag's EPC information, and 3) the maximum commu-

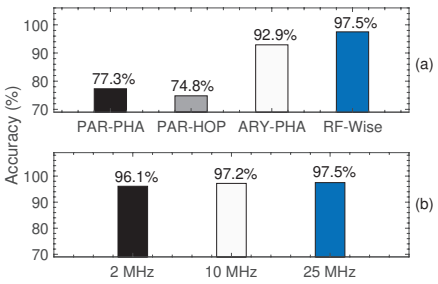

Fig. 14. Recognition accuracy (a) among different methods and (b) RF-Wise using various bandwidths.

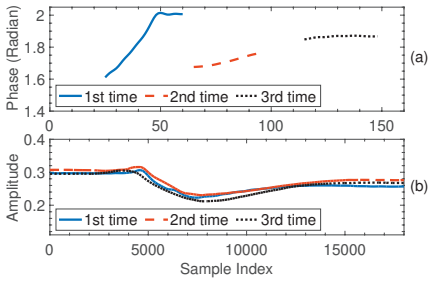

Fig. 15. The feature collected from three queries by using (a) frequency hopping and (b) RF-Wise.

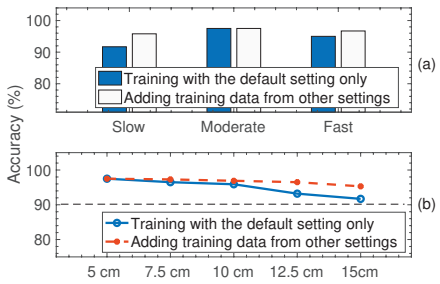

Fig. 16. Recognition accuracy v.s. (a) the gesture speed and (b) the hand-to-tag distance.

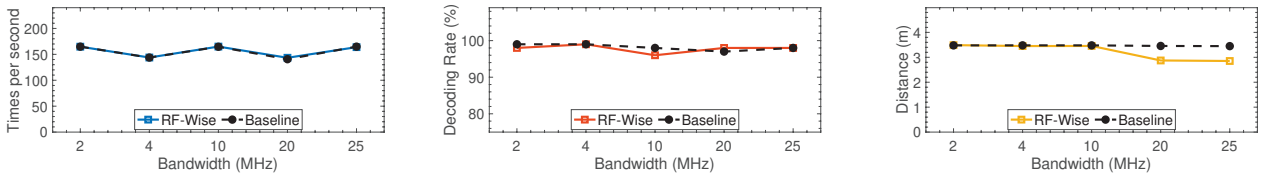

(a) Reading rate v.s. Bandwidth

(b) Decoding rate v.s. Bandwidth

(c) Reading distance v.s. Bandwidth

Fig. 17. Compatibility to the RFID communications.

nication distance (with the decoding rate higher than 97%). We can see that for each micro-benchmark, the performance of RF-Wise is similar to its baseline, which indicates that the customization of the RFID signals by RF-Wise does not impact the underlying RFID communications, while this design can bring powerful sensing abilities for RFID systems.

VI. Related Work

In existing RFID systems, reader can obtain accurate phase information from the RF signals, which are leveraged in many designs bounded to tag's own movements, *e.g.*, localization of tags [9], [32], [11], vibration counting [10], etc. However, it is not sufficient for a large spectrum of sensing tasks relying on the fine-grained features extracted from the RFID signals.

To advance RFID sensing, one representative family of solutions is to use a tag array of multiple tags and measure the RSS/phase/Doppler-shift information from these different tags to harness their features' spatial diversity [33]. In particular, GRfid [34] and RF-finger [29] use 35 and 40 tags to recognize different gestures. TagScan [13] adopts two linear tag arrays (eight tags for each array) for material sensing and shape imaging. EUIGR [35] and TagSMM [36] utilize four and six tags in their sensing designs. In addition to the deployment overhead by using multiple tags, the main drawback is the collision incurred among tags, which can easily degrade the sensing performance, especially to sense the moving target.

To overcome such limitations, recent works tend to use less tags and employ frequency hopping to increase the sensing fidelity across frequencies [12]. This principle works but the practical hurdle comes from the relatively large latency for hopping between two frequencies in RFID systems, *e.g.*, 200 ms. As shown in the evaluation, its improvement is limited, especially to sense the moving target. To advance prior sensing designs, some recent works [1], [27], [37] propose to introduce an extra device to transmit wideband (100∼500 MHz) signals during the RFID communication, so as to obtain multi-dimensional and high-resolution sensing information. However, the cost from such an extra transmitting device and the overhead to synchronize this extra signal with the RFID signal before the feature extraction cannot be neglected.

Different from these existing methods, RF-Wise can achieve fine-grained sensing samples cross different frequencies using one tag, which is a purely software-based solution without using any extra hardware. RF-Wise is motivated by an insightful observation to customize the RFID signals [38], [39], [40], while these works mainly add noises to secure RFID signals, which are not related to the frequency multiplexing and do not address the unique challenges encountered in RF-Wise. In the literature, there are also some RFID-based application designs, *e.g.*, authentication [41], temperature monitoring [42], beamforming [43], etc., which are orthogonal to this paper.

VII. Conclusion

This paper presents RF-Wise, a system to push the limit of RFID sensing. The key innovation is that through a purely software-based solution atop standard RFID using one tag, RF-Wise can obtain fine-grained CSI-like sensing samples across frequencies concurrently. Based on this, we further propose novel designs to ensure that the added sensing ability does not impact underlying RFID communications and make great engineering efforts in the development. We finally show the advantages of RF-Wise through two useful applications.

Acknowledgments

This work was supported by National Key R&D Program of China 2019YFB2102200, the GRF grant from Hong Kong RGC (CityU 11217420), the NSFC Grant No. 61832008, 62072367, 61772413, 61802299, 62002284, project funded by China Postdoctoral Science Foundation No.2021M692563. Zhenjiang Li is the corresponding author.

REFERENCES

[1] U. Ha, J. Leng, A. Khaddaj, and F. Adib, "Food and liquid sensing in practical environments using rfids," in *Proc. of USENIX NSDI*, 2020.

[2] Y. Xie, J. Xiong, M. Li, and K. Jamieson, "md-track: Leveraging multi-dimensionality for passive indoor wi-fi tracking," in *Proc. of ACM MobiCom*, 2019.

[3] Y. Wang, J. Shen, and Y. Zheng, "Push the limit of acoustic gesture recognition," in *Proc. of IEEE INFOCOM*, 2020.

[4] C. Occhiuzzi, S. Caizzone, and G. Marrocco, "Passive uhf rfid antennas for sensing applications: Principles, methods, and classifcations," *IEEE Antennas and Propagation Magazine*, 2013.

[5] F. Bibi, C. Guillaume, N. Gontard, and B. Sorli, "A review: Rfid technology having sensing aptitudes for food industry and their contribution to tracking and monitoring of food products," *Trends in Food Science & Technology*, 2017.

[6] S. Zhang, C. Yang, X. Kui, J. Wang, X. Liu, and S. Guo, "Reactor: Real-time and accurate contactless gesture recognition with rfid," in *Proc. of IEEE SECON*, 2019.

[7] Y.-M. Wang, Y.-S. Wang, and Y.-F. Yang, "Understanding the determinants of rfid adoption in the manufacturing industry," *Technological forecasting and social change*, 2010.

[8] EPCglobal, "Epc gen2," https://www.gs1.org/epcglobal.

[9] L. Yang, Y. Chen, X.-Y. Li, C. Xiao, M. Li, and Y. Liu, "Tagoram: Real-time tracking of mobile rfid tags to high precision using cots devices," in *Proc. of ACM MobiCom*, 2014.

[10] P. Li, Z. An, L. Yang, P. Yang, and Q. Lin, "Rfid harmonic for vibration sensing," *IEEE Transactions on Mobile Computing*, 2019.

[11] Y. Bu, L. Xie, Y. Gong, C. Wang, L. Yang, J. Liu, and S. Lu, "Rf-dial: An rfid-based 2d human-computer interaction via tag array," in *Proc. of IEEE INFOCOM*, 2018.

[12] B. Xie, J. Xiong, X. Chen, E. Chai, L. Li, Z. Tang, and D. Fang, "Tagtag: material sensing with commodity rfid," in *Proc. of ACM SenSys*, 2019.

[13] J. Wang, J. Xiong, X. Chen, H. Jiang, R. K. Balan, and D. Fang, "Tagscan: Simultaneous target imaging and material identification with commodity rfid devices," in *Proc. of ACM MobiCom*, 2017.

[14] M. Brain, T. V. Wilson, and B. Johnson, "How wifi works," *Dimuat turun Februari*, 2004.

[15] S. Kim, W.-C. Lee, S. Ahn, and S. Choi, "Design of cic roll-off compensation filter in a w-cdma digital if receiver," *Digital Signal Processing*, 2006.

[16] N. Kargas, F. Mavromatis, and A. Bletsas, "Fully-coherent reader with commodity sdr for gen2 fm0 and computational rfid," *IEEE Wireless Communications Letters*, 2015.

[17] "Rf-wise," https://cui-zhao.github.io/RF-WISE/.

[18] Alcohol and you, "The dangers of fake alcohol," https://www.alcoholandyouni.com/the-dangers-of-fake-alcohol/.

[19] T. Atlantic, "Fake medicine is a bigger problem than you think," https://www.theatlantic.com/sponsored/pfizer-2017/need-to-know-fake-medicine-is-a-bigger-problem-than-you-think/1610/.

[20] U. Ha, Y. Ma, Z. Zhong, T.-M. Hsu, and F. Adib, "Learning food quality and safety from wireless stickers," in *Proc. of ACM Workshop on HotNets*, 2018.

[21] Y. Yang, G. D. Clark, J. Lindqvist, and A. Oulasvirta, "Free-form gesture authentication in the wild," in *Proc. of ACM CHI*, 2016.

[22] W. Wang, A. X. Liu, M. Shahzad, K. Ling, and S. Lu, "Understanding and modeling of wifi signal based human activity recognition," in *Proc. of ACM MobiCom*, 2015.

[23] H. Xianren, Z. Dongyan, T. Xiaoke, L. Dejian, F. Xi, and S. Hongwei, "A uhf rfid communication link rate adjustment strategy and implementation," in *Proc. of IEEE ICECE*, 2020.

[24] C. Xing, N. Wang, J. Ni, Z. Fei, and J. Kuang, "Mimo beamforming designs with partial csi under energy harvesting constraints," *IEEE Signal Processing Letters*, 2013.

[25] M. P. Donadio, "Cic filter introduction," in *Proc. of IEEE ISC*, 2000.

[26] G. J. Dolecek and F. Harris, "On design of two-stage cic compensation filter," in *Proc. of IEEE ISIE*, 2009.

[27] Z. Luo, Q. Zhang, Y. Ma, M. Singh, and F. Adib, "3d backscatter localization for fine-grained robotics," in *Proc. of USENIX NSDI*, 2019.

[28] E. Research, "About usrp bandwidths and sampling rates," https://kb.ettus.com/About_USRP_Bandwidths_and_Sampling_Rates.

[29] C. Wang, J. Liu, Y. Chen, H. Liu, L. Xie, W. Wang, B. He, and S. Lu, "Multi-touch in the air: Device-free finger tracking and gesture recognition via cots rfid," in *Proc. of IEEE INFOCOM*, 2018.

[30] M. Hall, E. Frank, G. Holmes, B. Pfahringer, P. Reutemann, and I. H. Witten, "The weka data mining software: an update," *ACM SIGKDD explorations newsletter*, 2009.

[31] G. Wang, J. Han, C. Qian, W. Xi, H. Ding, Z. Jiang, and J. Zhao, "Verifiable smart packaging with passive rfid," *IEEE Transactions on Mobile Computing*, 2018.

[32] L. Shangguan, Z. Yang, A. X. Liu, Z. Zhou, and Y. Liu, "Stpp: Spatial-temporal phase profiling-based method for relative rfid tag localization," *IEEE/ACM Transactions on Networking*, 2016.

[33] S. R. Banerjee, R. Jesme, and R. A. Sainati, "Investigation of spatial and frequency diversity for long range uhf rfid," in *Proc. of IEEE APS*, 2008.

[34] Y. Zou, J. Xiao, J. Han, K. Wu, Y. Li, and L. M. Ni, "Grfid: A device-free rfid-based gesture recognition system," *IEEE Transactions on Mobile Computing*, 2016.

[35] Y. Yu, D. Wang, R. Zhao, and Q. Zhang, "Rfid based real-time recognition of ongoing gesture with adversarial learning," in *Proc. of ACM SenSys*, 2019.

[36] B. Xie, J. Xiong, X. Chen, and D. Fang, "Exploring commodity rfid for contactless sub-millimeter vibration sensing," in *Proc. of ACM SenSys*, 2020.

[37] Y. Ma, N. Selby, and F. Adib, "Minding the billions: Ultra-wideband localization for deployed rfid tags," in *Proc. of ACM MobiCom*, 2017.

[38] Y. Yang, J. Cao, and X. Liu, "Er-rhythm: Coupling exercise and respiration rhythm using lightweight cots rfid," *Proceedings of the ACM on Interactive, Mobile, Wearable and Ubiquitous Technologies*, 2019.

[39] G. Wang, H. Cai, C. Qian, J. Han, X. Li, H. Ding, and J. Zhao, "Towards replay-resilient rfid authentication," in *Proc. of ACM MobiCom*, 2018.

[40] H. Hassanieh, J. Wang, D. Katabi, and T. Kohno, "Securing rfids by randomizing the modulation and channel," in *Proc. of USENIX NSDI*, 2015.

[41] C. Zhao, Z. Li, T. Liu, H. Ding, J. Han, W. Xi, and R. Gui, "Rf-mehndi: A fingertip profiled rf identifier," in *Proc. of IEEE INFOCOM*, 2019.

[42] S. Pradhan and L. Qiu, "Rtsense: passive rfid based temperature sensing," in *Proc. of ACM SenSys*, 2020.

[43] J. Wang, J. Zhang, R. Saha, H. Jin, and S. Kumar, "Pushing the range limits of commercial passive rfids," in *Proc. of USENIX NSDI*, 2019.